Lewis Acid Enhancement of Proton Induced CO₂ Cleavage: Bond

Joshua A. Buss, David G. VanderVelde, and Theodor Agapie*

Weakening and Ligand Residence Time Effects

Division of Chemistry and Chemical Engineering, California Institute of Technology, 1200 E. California Boulevard MC 127-72, Pasadena, California 91125, United States

Supporting Information

ABSTRACT: Though Lewis acids (LAs) have been shown to have profound effects on carbon dioxide (CO₂) reduction catalysis, the underlying cause of the improved reactivity remains unclear. Herein, we report a well-defined molecular system for probing the role of LA additives in the reduction of CO2 to carbon monoxide (CO) and water. Mo(0) CO₂ complex (2) forms adducts with a series of LAs, demonstrating CO2 activation that correlates linearly with the strength of the LA. Protons induce C-O cleavage of these LA adducts, in contrast to the CO₂ displacement primarily observed in the absence of LA. CO2 cleavage shows dependence on both bond activation and the residence time of the bound small molecule, demonstrating the influence of both kinetic and thermodynamic factors on promoting productive CO2 reduction chemistry.

As the terminal product of fossil fuel combustion, the conversion of carbon dioxide (CO₂) to energy-dense, liquid fuels is a necessary step in closing an anthropogenic carbon cycle. Technologies for the capture, copolymerization,³ and hydrogenation⁴ of CO₂ have recently emerged, and their study and design is topical. However, the controlled reduction of CO2 with protons and electrons is most relevant to artificial photosynthesis and couples most directly to the storage of renewable energy in chemical bonds. 1d,5 Because of the kinetic stability of $CO_{2^{\prime}}^{-6}$ the range of products formed in a narrow potential window, and competing reduction reactions, 5b,8 efficient and robust catalysts capable of the selective reduction of CO₂ remain a subject of significant interest.^{6a}

In nature, the two-electron two-proton reduction of CO₂ is executed reversibly by CO-dehydrogenases (CODH). The enzyme active site of NiFe-CODH features a redox active Ni center and an Fe(III) ion that coordinate CO_2 in a μ - η C: η O binding motif (Figure 1).9b Added Lewis acids (LAs) likewise promote rate enhancements and redox potential shifts in electrocatalytic CO₂ reduction. This strategy of cooperative CO₂ activation has inspired molecular mimics in the form of ligand scaffolds that feature LAs in the coordination sphere, 11 heterobimetallic complexes, ¹² exogenous LA addition to CO₂ bound metal complexes or CO₂ reduction intermediates, ^{9a,13} and reduction catalysis combining transition metals and diboranes.¹⁴ Though LAs are capable of promoting CO₂ binding^{9a} and increasing the degree of CO₂ activation, ^{13c} systematic investigations of their effect on reactivity of the

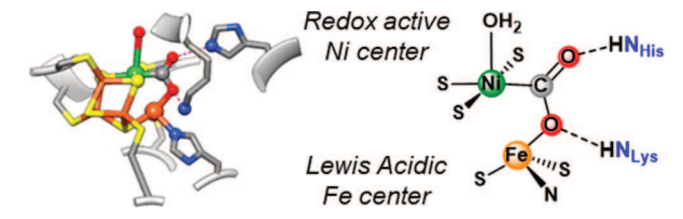


Figure 1. Solid-state structure (left, PDB: 4UDX)⁷ and schematic representation (right) of the CO₂-bound NiFe-CODH active site.

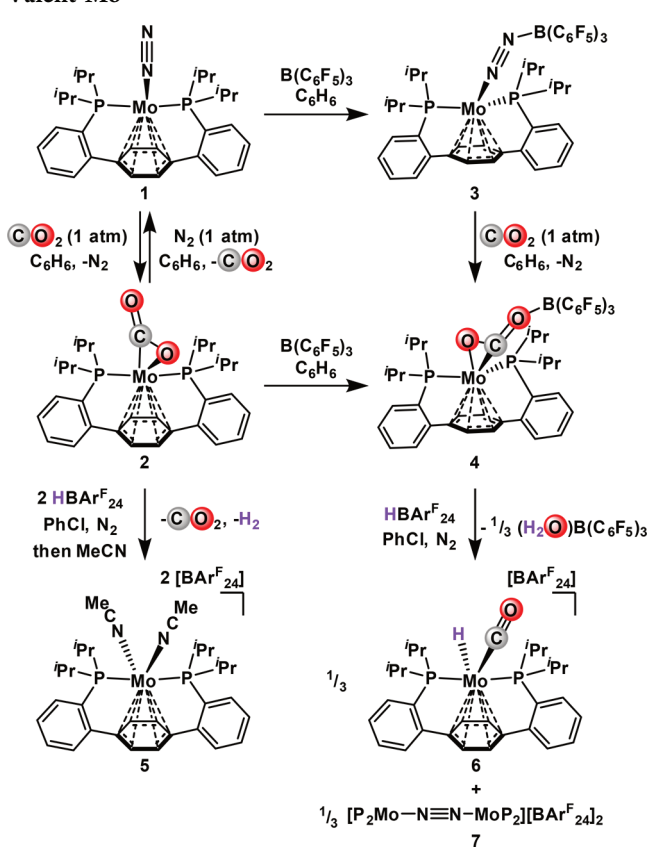
bound CO2 unit remain scant. Herein, we describe a study correlating Lewis acidity and the degree of CO2 activation in a low-valent Mo complex. 15 Moreover, we demonstrate that LA addition facilitates C-O bond cleavage, chemistry that does not proceed from the parent LA-free CO2 complex, via both kinetic stabilization and increased small molecule activation.

Dinitrogen adduct 1 reversibly binds CO2, resulting in formation of an η^2 -CO₂ complex, 2 (Scheme 1). Under an atmosphere of ¹³CO₂, the ³¹P{¹H} and ¹³C{¹H} NMR spectra display a coupling doublet and triplet at 62.8 and 192.4 ppm $(^{2}J(C,P) = 29.3 \text{ Hz})$, respectively, consistent with coordination of a single ¹³CO₂ molecule. ¹⁶ The IR spectrum of 2 displays stretches at 1716 and 1198 cm⁻¹, sensitive to ¹²C/¹³C isotopic labeling, again supporting a bound CO₂ motif. 16,17 Solid-state analysis of single crystals of 2 grown under a CO₂ atmosphere confirm the η^2 binding mode (Figure 2).

Interested in the thermodynamics of this reversible small molecule binding, longitudinal relaxation (T1) times were measured for the relevant ¹³C and ¹⁵N resonances of an equilibrium mixture of 1-¹⁵N, 2-¹³C, ¹⁵N₂ and ¹³CO₂. Uncharacteristically short values were observed for 1^{-15} N, free 15 N₂, 2^{-13} C, and free 13 CO₂—5.1(4), 4.9(3), 12.5(4), and 16.8(7) s, respectively. These short and near equivalent T_1 times suggest an exchange process that enables new relaxation pathways unavailable to the free small molecules. 19 In the case of CO₂, exchange was confirmed by magnetization transfer. The high lability of the CO₂ ligand was reflected in the reactivity of 2. Addition of excess acid to 2 at room temperature resulted in CO2 dissociation and formation of Mo(II) dication 5 (Scheme 1), via a Mo hydride cation,²⁰ which has been observed in stoichiometric reactions with acid. In CO2 reduction electrocatalysis, conversion to the metal hydride moves selectivity away from CO, affording either

Received: June 8, 2018 Published: July 23, 2018 Journal of the American Chemical Society

Scheme 1. CO_2 Binding and LA Adduct Formation at Low-Valent \mathbf{Mo}^{\sharp}



 ‡ HBAr $^{F}_{24}$ = [H(Et₂O)₂][BAr $^{F}_{24}$] (BAr $^{F}_{24}$ = tetrakis[3,5-bis-(trifluoromethyl)phenyl]borate).

formate or H_2 , and representing a branching point in terms of defining the selectivity of CO_2 reduction. Despite its implication as a critical step in CO_2 to CO reduction catalysis, there is a paucity of reports of the protonation of well-defined CO_2 adducts of transition metals. Indeed, protolytic dissociation and subsequent gas analysis was a common characterization technique for metal- CO_2 complexes.

Borane LAs have been employed to activate metal coordinated small molecules. 13a,c,25 Addition of the strong

LA tris(pentafluorophenyl)borane (B(C_6F_5)₃) to complex 1 affords the LA/base adduct 3 (Scheme 1), as confirmed by XRD (Figure 2). The bond metrics of complex 3 are consistent with significant activation of the N₂ unit.²⁶ The solid-state IR spectrum corroborates weakening of the N–N bond, with the stretch red shifting by 134 cm⁻¹. NMR spectroscopy supports a strong borane/nitrogen interaction in solution, with both the ¹⁹F (-135.0, -157.9, and -166.8 ppm)²⁷ and ¹¹B (-14.4 ppm)²⁸ spectra consistent with four-coordinate boron.

Treating 3 with CO_2 , or 2 with $B(C_6F_5)_3$, results in the formation of a new LA adduct, 4, quantitatively. Contrasting the equilibrium between complexes 1 and 2, which slightly favors N_2 binding ($K_{eq} = 0.48$), addition of $B(C_6F_5)_3$ renders CO_2 binding irreversible (Scheme 1), likely a consequence of the strong B–O interaction; 4 is stable under N_2 in both the solid-state and solution. The triplet for the $^{13}CO_2$ unit of isotopically labeled 4- ^{13}C moves downfield relative to 2 (218.9 ppm, C_6D_6) and exhibits smaller $^2J(C,P)$ scalar coupling (11.47 Hz). Akin to 3, the ^{11}B and ^{19}F NMR data are consistent with four-coordinate boron.

The solid-state structure of 4 exhibits a μ - η^2 C,O: η O bridging CO₂ unit between Mo and B (Figure 2). Borane binding to metal-coordinated CO₂ is rare, but 4 displays similar bond metrics to such complexes. The structural parameters are consistent with significant CO₂ activation, a phenomenon also borne out in the IR spectrum. The stretches for the CO₂ unit shift to 1602 and 1218 cm⁻¹, as confirmed by isotopic labeling.

When stabilized with a LA, the reactivity of the Mo $\rm CO_2$ complex is decidedly different. The reaction of 4-¹³C with HBAr^F₂₄ results in the formation of a single diamagnetic Mo complex (Scheme 1). The ³¹P{¹H} and ¹³C{¹H} NMR spectra display a doublet (92.64 ppm) and triplet (220.08 ppm), respectively ($^2J(P,C) = 14.6$ Hz), consistent with $\rm CO_2$ cleavage to a metal-bound carbonyl. The identity of this product was confirmed as carbonyl hydride cation, 6-¹³C, via XRD and independent synthesis.²⁹

A balanced reaction for the formation of **6** requires a reductant. When run under N_2 , the electrons are provided by **1**, which is generated under the reaction conditions upon borane displacement. Concomitantly with generation of **6**, a paramagnetic $Mo(I)-N_2-Mo(I)$ dinuclear complex, **7**, is formed, as confirmed by XRD. Quantifying conversion to **6** shows ca. 33% C-O cleavage, consistent with a process

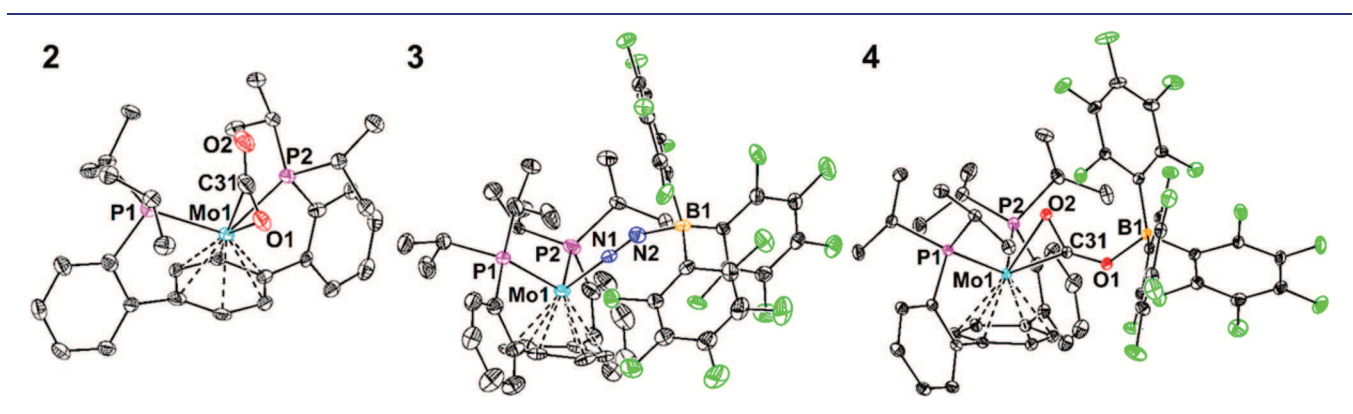


Figure 2. Solid-state structures of complexes 2–4. Thermal anisotropic displacement ellipsoids are shown at the 50% probability level. H atoms are omitted for clarity. Selected bond distances [Å] and angles $[^{\circ}]$ —3: Mo1–N1 1.913(2), N1–N2 1.163(3), N2–B1 1.585(37), \angle Mo1–N1–N2 179.1(3), \angle N1–N2–B1 158.2(1.2); 4: Mo1–O2 2.2535(6), Mo1–C31 2.0574(8), O2–C31 1.246(1), C31–O1 1.275(1), O1–B1 1.554(1), \angle O2–C31–O1 130.93(8), \angle C31–O1–B1 132.13(7).

involving 1 acting as a single electron reductant; one electron oxidation of 1 with [Fc][BArF₂₄] likewise provides 7. Borane speciation in the protonation reactions was tracked by ¹⁹F NMR spectroscopy, supporting formation of a bis(borane) hydroxide³⁰ and subsequent protonation to a borane aquo adduct.31 Remarkably, LA coordination "turns on" C-O cleavage chemistry, affording CO and H₂O from CO₂ and acid. Borane binding facilitates the delocalization of electron density from the low-valent Mo center into the LUMO of CO2, in a push-pull mechanism, similar to the "bifunctional attack" proposed for NiFe-CODH.

Interested in the generality of the CO2 activation observed upon LA coordination to 2, a series of alkali metal $(Na(BAr_{24}^F))$ and $Cs(BAr_{24}^F)$ and borane $(B(C_6H_2F_3)_3)$ $B(C_6F_5)_3$, and $B(C_6H_3(CF_3)_2)_3$) LAs were added to 2-13 C. In each case, ${}^{13}C\{{}^{1}H\}$ and ${}^{31}P\{{}^{1}H\}$ NMR spectroscopies supported adduct formation, displaying resonances shifted downfield and upfield, respectively, from those of 2 (Tables 1

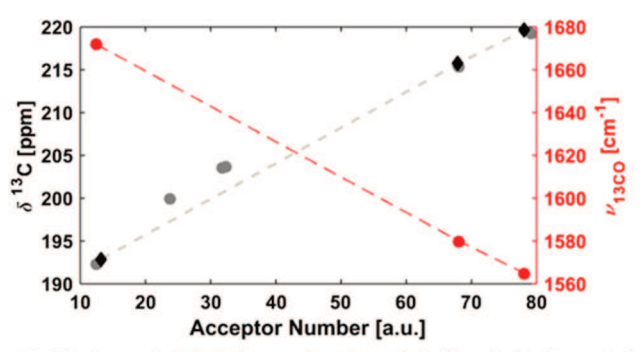
Table 1. CO₂ Activation, Exchange Rate, and Cleavage Data

					% CO Cleavage	
	LA	AN	δ^{13} C (ppm)	$Rate \times 10^{-6}$ (s^{-1})	Abs ^a	Rel ^b
PhCl/ Et ₂ O	None	12.4	192.3	>200 ^c	0	0
	Cs(BArF ₂₄)	23.7	199.9	20	7	21
	Na(BArF ₂₄)	31.8	203.5	6	4	12
	$Na(BAr^{F}_{24})^{d}$	32.4	203.7	2	5	15
	$B(C_6H_2F_3)_3$	68.1	215.3	5	4	12
	$B(C_6F_5)_3$	79.2	219.3	9	9	18
PhCl	None	13.2	192.9	>200 ^c	1	3
				>70 ^e	10 ^f	30 ^f
	$B(C_6H_2F_3)_3$	67.9	215.7	2	13	39
	$B(C_6F_5)_3$	78.1	219.6	2	17	51
					33 ^g	99 ^g
	$\frac{B(C_6H_{3^-})}{(CF_3)_2}$	82.7	219.1	1	16	48

^aDetermined by relative integration (³¹P NMR spectroscopy) against a Ph₃P=O internal standard. ^bRelative to a theoretical maximum of 33%. ^cIsotope equilibration was too rapid for accurate determination of the rate. ^dThe [Na(BAr^F₂₄)] was doubled. ^eMeasured at -13 °C. ^fAcid was added immediately upon thawing of the reaction solution. g1 equiv of HBArF24 was added.

and S2). The degree of CO₂ activation, as reported by the ¹³C chemical shift, trends linearly with the strength of the LA, as quantified by the acceptor number (AN, Figure 3).³² A similar linear trend is seen when comparing AN vs $\nu_{\rm CO2}$, 33 suggesting that, in this case, the ¹³C chemical shift of the bound CO₂ ligand correlates with the degree of C-O bond activation.

Revisiting protonation with these new LA adducts (Scheme 2),34 we were gratified to see that in all cases, C-O bond cleavage was enhanced (Table 1). The extent of C-O cleavage³⁵ in PhCl/Et₂O³⁶ increased to roughly the same level, in the rage of 4-9%, and not proportionally with the LA AN. Changing to neat PhCl resulted in a further increase to bond cleavage up to 13-16%. Importantly, a 2-fold increase in formation of 6^{-13} C is observed for $B(C_6H_2F_3)_3$ and $B(C_6F_5)_3$ adducts of 2-13C, despite little perturbation in their respective ¹³C NMR chemical shifts between the two solvent systems. These data are inconsistent with the hypothesis that C-O activation alone controls CO2 reduction chemistry.



The ¹³C chemical shift of the CO₂ ligand, in PhCl (図) and PhCl/Et₂O (◎), tracks inversely with the C-O stretching frequency (.).

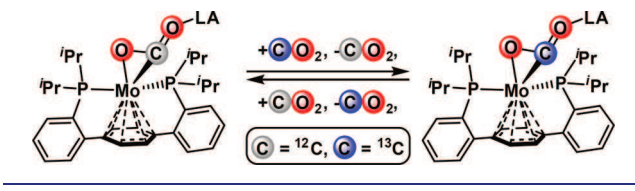
Figure 3. CO₂ Activation as a function of Lewis Acidity.

Scheme 2. Protonation of in Situ Formed LA Adducts



We next investigated the kinetics of degenerate CO2 exchange as a measure for the impact of LA binding on the lability of the Mo-CO₂ interaction (Scheme 3). Exposing

Scheme 3. CO₂ Self-Exchange in Mo-CO₂ LA Adducts



solutions of 2-13C and a LA additive to an excess of 12CO2 at 0 °C, resulted in decay of the resonance associated with bound CO₂ in the ¹³C{¹H} NMR spectrum, providing a handle for kinetic analysis. The LA-free exchange rate is over 2 orders of magnitude faster than those of the LA-stabilized adducts. However, a systematic dependence of the exchange rates on the strength of the added LA was not observed (Table 1). The exchange rates are similar for most of the LAs, irrespective of their AN or the ¹³C chemical shift of the adduct they form.

Some trends are evident from the combined kinetic data (Table 1). Borane LA adducts exchange CO2 marginally faster in the presence of Et₂O, a competing Lewis base, supporting LA dissociation as a rate effecting step. Likewise, increasing the concentration of LA slows self-exchange, further corroborating a mechanism involving LA dissociation. For the same concentration of LA, the exchange rates are all quite similar and significantly slower than in the absence of LA. The promotion of C-O cleavage in LA adducts correlates with this kinetic factor, the "residence time" of the CO2 adduct, or the propensity of the substrate to remain coordinated to the metal center, not simply to the degree of CO₂ activation. Further highlighting the importance of kinetic stabilization, C-O cleavage was observed in the absence of LA when protonation was performed at low temperature (Table 1). CO₂ selfexchange likewise showed a significant dampening upon cooling, while the degree of C-O activation does not change. These data suggest that increased residence time of CO₂ at Mo, a consequence of the push-pull interaction, is instrumental for bond cleavage. A competing mechanism for protonation at Mo upon CO_2 dissociation erodes selectivity for CO_2 activation. In terms of augmenting the C-O cleavage preference, increasing the residence time is a decisive factor, independent of the mode of tuning it (temperature vs LA binding).

In summary, a labile Mo(0) CO_2 adduct interacts with a variety of LAs, increasing both the degree of activation and the kinetic stability of bound CO_2 . LA addition enhances proton-induced cleavage to CO and H_2O , chemistry that correlates inversely with the kinetics of CO_2 exchange. This work establishes the residence time of a small molecule substrate in the coordination sphere of the metal as a critical factor in engendering desirable transformation chemistry of labile substrates. LAs additives are shown to improve CO_2 cleavage by kinetic stabilization, not simply thermodynamic activation.

ASSOCIATED CONTENT

S Supporting Information

The Supporting Information is available free of charge on the ACS Publications website at DOI: 10.1021/jacs.8b05874.

Crystallographic details (CIF)

Detailed experimental procedures, full characterization, and spectroscopic data (PDF)

AUTHOR INFORMATION

Corresponding Author

*agapie@caltech.edu

ORCID ®

Theodor Agapie: 0000-0002-9692-7614

Notes

The authors declare no competing financial interest.

ACKNOWLEDGMENTS

We thank Larry Henling and Mike Takase for invaluable crystallographic assistance. T.A. is grateful for a Dreyfus fellowship and J.A.B. for a NSF graduate research fellowship. We thank the NSF (CHE-1151918 and CHE-1800501), the Dow Next Generation Education Fund (for instrumentation at Caltech), and Caltech for funding.

REFERENCES

- (1) (a) Liu, Q.; Wu, L.; Jackstell, R.; Beller, M. Nat. Commun. 2015, 6, 5933. (b) Aresta, M.; Dibenedetto, A.; Angelini, A. Chem. Rev. 2014, 114, 1709. (c) Appel, A. M.; Bercaw, J. E.; Bocarsly, A. B.; Dobbek, H.; DuBois, D. L.; Dupuis, M.; Ferry, J. G.; Fujita, E.; Hille, R.; Kenis, P. J. A.; Kerfeld, C. A.; Morris, R. H.; Peden, C. H. F.; Portis, A. R.; Ragsdale, S. W.; Rauchfuss, T. B.; Reek, J. N. H.; Seefeldt, L. C.; Thauer, R. K.; Waldrop, G. L. Chem. Rev. 2013, 113, 6621. (d) Olah, G. A.; Prakash, G. K. S.; Goeppert, A. J. Am. Chem. Soc. 2011, 133, 12881. (e) Aresta, M.; Dibenedetto, A. Dalton Trans. 2007, 2975.
- (2) (a) Belmabkhout, Y.; Guillerm, V.; Eddaoudi, M. Chem. Eng. J. 2016, 296, 386. (b) Schoedel, A.; Ji, Z.; Yaghi, O. M. Nature Energy 2016, 1, 16034. (c) Leung, D. Y. C.; Caramanna, G.; Maroto-Valer, M. M. Renewable Sustainable Energy Rev. 2014, 39, 426.
- (3) (a) Zhang, X.; Fevre, M.; Jones, G. O.; Waymouth, R. M. Chem. Rev. 2018, 118, 839. (b) Sakakura, T.; Choi, J.-C.; Yasuda, H. Chem. Rev. 2007, 107, 2365. (c) Coates, G. W.; Moore, D. R. Angew. Chem., Int. Ed. 2004, 43, 6618.
- (4) (a) Sordakis, K.; Tang, C.; Vogt, L. K.; Junge, H.; Dyson, P. J.; Beller, M.; Laurenczy, G. Chem. Rev. 2018, 118, 372. (b) Bernskoetter,

- W. H.; Hazari, N. Acc. Chem. Res. 2017, 50, 1049. (c) Mellmann, D.; Sponholz, P.; Junge, H.; Beller, M. Chem. Soc. Rev. 2016, 45, 3954. (d) Bielinski, E. A.; Lagaditis, P. O.; Zhang, Y.; Mercado, B. Q.; Würtele, C.; Bernskoetter, W. H.; Hazari, N.; Schneider, S. J. Am. Chem. Soc. 2014, 136, 10234.
- (5) (a) Costentin, C.; Robert, M.; Saveant, J.-M. Chem. Soc. Rev. **2013**, 42, 2423. (b) Benson, E. E.; Kubiak, C. P.; Sathrum, A. J.; Smieja, J. M. Chem. Soc. Rev. **2009**, 38, 89. (c) Rakowski Dubois, M.; Dubois, D. L. Acc. Chem. Res. **2009**, 42, 1974.
- (6) (a) Grice, K. A. Coord. Chem. Rev. 2017, 336, 78. (b) Paparo, A.; Okuda, J. Coord. Chem. Rev. 2017, 334, 136.
- (7) Fesseler, J.; Jeoung, J.-H.; Dobbek, H. Angew. Chem., Int. Ed. 2015, 54, 8560.
- (8) Qiao, J.; Liu, Y.; Hong, F.; Zhang, J. Chem. Soc. Rev. 2014, 43, 631.
- (9) (a) Forrest, S. J. K.; Clifton, J.; Fey, N.; Pringle, P. G.; Sparkes, H. A.; Wass, D. F. *Angew. Chem., Int. Ed.* **2015**, *54*, 2223. (b) Jeoung, J.-H.; Dobbek, H. *Science* **2007**, *318*, 1461.
- (10) (a) Sampson, M. D.; Kubiak, C. P. J. Am. Chem. Soc. **2016**, 138, 1386. (b) Bhugun, I.; Lexa, D.; Savéant, J.-M. J. Phys. Chem. **1996**, 100, 19981. (c) Hammouche, M.; Lexa, D.; Momenteau, M.; Saveant, J. M. J. Am. Chem. Soc. **1991**, 113, 8455.
- (11) (a) Takaya, J.; Iwasawa, N. J. Am. Chem. Soc. 2017, 139, 6074. (b) Cammarota, R. C.; Vollmer, M. V.; Xie, J.; Ye, J.; Linehan, J. C.; Burgess, S. A.; Appel, A. M.; Gagliardi, L.; Lu, C. C. J. Am. Chem. Soc. 2017, 139, 14244. (c) Devillard, M.; Declercq, R.; Nicolas, E.; Ehlers, A. W.; Backs, J.; Saffon-Merceron, N.; Bouhadir, G.; Slootweg, J. C.; Uhl, W.; Bourissou, D. J. Am. Chem. Soc. 2016, 138, 4917.
- (12) (a) Bagherzadeh, S.; Mankad, N. P. J. Am. Chem. Soc. 2015, 137, 10898. (b) Krogman, J. P.; Foxman, B. M.; Thomas, C. M. J. Am. Chem. Soc. 2011, 133, 14582.
- (13) (a) Yoo, C.; Lee, Y. Chem. Sci. 2017, 8, 600. (b) Rauch, M.; Parkin, G. J. Am. Chem. Soc. 2017, 139, 18162. (c) Kim, Y.-E.; Kim, J.; Lee, Y. Chem. Commun. 2014, 50, 11458. (d) Jiang, Y.; Blacque, O.; Fox, T.; Berke, H. J. Am. Chem. Soc. 2013, 135, 7751.
- (14) (a) Jin, G.; Werncke, C. G.; Escudié, Y.; Sabo-Etienne, S.; Bontemps, S. J. Am. Chem. Soc. 2015, 137, 9563. (b) Chakraborty, S.; Zhang, J.; Krause, J. A.; Guan, H. J. Am. Chem. Soc. 2010, 132, 8872. (c) Laitar, D. S.; Müller, P.; Sadighi, J. P. J. Am. Chem. Soc. 2005, 127, 17196.
- (15) Mo complexes have been employed previously for $\rm CO_2$ reduction chemistry. For select examples, see: (a) Zhang, Y.; Williard, P. G.; Bernskoetter, W. H. *Organometallics* **2016**, *35*, 860. (b) Neary, M. C.; Parkin, G. *Chem. Sci.* **2015**, *6*, 1859. (c) Clark, M. L.; Grice, K. A.; Moore, C. E.; Rheingold, A. L.; Kubiak, C. P. *Chem. Sci.* **2014**, *5*, 1894.
- (16) (a) Carden, R. G.; Ohane, J. J.; Pike, R. D.; Graham, P. M. Organometallics 2013, 32, 2505. (b) Bernskoetter, W. H.; Tyler, B. T. Organometallics 2011, 30, 520. (c) Contreras, L.; Paneque, M.; Sellin, M.; Carmona, E.; Perez, P. J.; Gutierrez-Puebla, E.; Monge, A.; Ruiz, C. New J. Chem. 2005, 29, 109. (d) Alvarez, R.; Carmona, E.; Marin, J. M.; Poveda, M. L.; Gutierrez-Puebla, E.; Monge, A. J. Am. Chem. Soc. 1986, 108, 2286.
- (17) Gambarotta, S.; Floriani, C.; Chiesi-Villa, A.; Guastini, C. J. Am. Chem. Soc. 1985, 107, 2985.
- (18) (a) Seravalli, J.; Ragsdale, S. W. Biochemistry **2008**, 47, 6770. (b) We could not find a reported T_1 time for N_2 gas in organic solvent. There are, however, extensive studies on ^{15}N relaxation parameters at low temperature in liquid N_2 . See: Ishol, L. M.; Scott, T. A.; Goldblatt, M. J. Magn. Reson. **1976**, 23, 313.
- (19) Ishol, L. M.; Scott, T. A.; Goldblatt, M. J. Magn. Reson. 1976, 23, 313.
- (20) Buss, J. A.; Edouard, G. A.; Cheng, C.; Shi, J.; Agapie, T. J. Am. Chem. Soc. 2014, 136, 11272.
- (21) Schneider, J.; Jia, H.; Muckerman, J. T.; Fujita, E. Chem. Soc. Rev. 2012, 41, 2036.
- (22) (a) Chapovetsky, A.; Do, T. H.; Haiges, R.; Takase, M. K.; Marinescu, S. C. *J. Am. Chem. Soc.* **2016**, *138*, 5765. (b) Sampson, M. D.; Nguyen, A. D.; Grice, K. A.; Moore, C. E.; Rheingold, A. L.;

- Kubiak, C. P. J. Am. Chem. Soc. 2014, 136, 5460. (c) Bhugun, I.; Lexa,
 D.; Savéant, J.-M. J. Am. Chem. Soc. 1996, 118, 1769. (d) DuBois, D.
 L.; Miedaner, A.; Haltiwanger, R. C. J. Am. Chem. Soc. 1991, 113, 8753. (e) Ishida, H.; Tanaka, K.; Tanaka, T. Organometallics 1987, 6, 181.
- (23) (a) Sahoo, D.; Yoo, C.; Lee, Y. J. Am. Chem. Soc. **2018**, 140, 2179. (b) Tsai, J. C.; Khan, M.; Nicholas, K. M. Organometallics **1989**, 8, 2967.
- (24) Vol'pin, M. E.; Kolomnikov, I. S. Pure Appl. Chem. 1973, 33, 567
- (25) (a) Geri, J. B.; Shanahan, J. P.; Szymczak, N. K. J. Am. Chem. Soc. 2017, 139, 5952. (b) Simonneau, A.; Turrel, R.; Vendier, L.; Etienne, M. Angew. Chem., Int. Ed. 2017, 56, 12268.
- (26) The N1–N2 distance elongates by 0.06 Å and the N2–B distance, at 1.586(5) Å, is similar to that of a reported borane N_2 adduct (see ref 25a).
- (27) (a) Parks, D. J.; Piers, W. E.; Yap, G. P. A. Organometallics 1998, 17, 5492. (b) Horton, A. D.; de With, J. Organometallics 1997, 16, 5424.
- (28) Lewiński, J.; Kubicki, D. In *Encyclopedia of Spectroscopy and Spectrometry*, Third Edition; Tranter, G. E., Koppenaal, D. W., Eds.; Academic Press: Oxford, 2017; p 318.
- (29) Cation 6 is accessible via addition of HBAr^F₂₄ to a Mo(0) monocarbonyl complex (Scheme S1).
- (30) Xu, T.; Chen, E. Y. X. J. Am. Chem. Soc. 2014, 136, 1774.
- (31) Bergquist, C.; Bridgewater, B. M.; Harlan, C. J.; Norton, J. R.; Friesner, R. A.; Parkin, G. *J. Am. Chem. Soc.* **2000**, *122*, 10581.
- (32) Beckett, M. A.; Strickland, G. C.; Holland, J. R.; Sukumar Varma, K. *Polymer* **1996**, *37*, 4629.
- (33) Even with isotopic enrichment, the C-O stretches of the alkali metal LA adducts were inadequately resolved to be assigned with confidence. This limits the available IR data to three points; however, a clear linear trend is observed for both the ¹²C and ¹³C isotoplogues.
- (34) These reactions were performed with strict exclusion of \tilde{N}_2 to avoid potential exchange prior to protonation.
- (35) The theoretical maximum of which is 33% (vide supra).
- (36) Protonation experiments were performed in a 2 PhCl:1 Et₂O solvent mixture, which solubilizes both alkali metal and borane LAs and their adducts.